HEMICELLULOSE GLUCOXYLAN FROM *MIMOSA PUDICA* SEEDS AS A GREEN REDUCING AND STABILIZING AGENT FOR ZINC OXIDE NANOPARTICLES WITH ANTIMICROBIAL AND WOUND HEALING ACTIVITIES

MANAHIL NOOR,[*] MARYAM NASEER,[**] NIMRA ARIF,[**]
MUHAMMAD UMAIR SHARIF,[*] TUBA TUBA,[*] GULZAR MUHAMMAD,[*] IQRA UROOJ,[*]
MUHAMMAD ARSHAD RAZA[*] and ADNAN ASHRAF[***]

[*]*Department of Chemistry, Institute of Chemical Sciences, Government College University Lahore, 54000 Lahore, Pakistan*
[**]*Department of Chemistry and Chemical Engineering, Syed Babar Ali School of Science and Engineering (SBASSE), Lahore University of Management Sciences (LUMS), Lahore, 54792 Pakistan*
[***]*Department of Chemistry, University of Lahore, Raiwind Road, Lahore, Pakistan*
✉ *Corresponding author: G. Muhammad, mgulzar@gcu.edu.pk*

Received November 1, 2025

In the present study, zinc oxide nanoparticles (ZnO NPs) were synthesized using glucoxylan (GX), a hemicellulose derived from *Mimosa pudica* seeds. The UV-visible spectrum displayed an intense absorption peak at 390 nm, while FTIR spectra revealed two characteristic Zn-O stretching bands at 441 and 484 cm^{-1}. SEM, XRD, and EDX analyses revealed predominantly spherical particles (51.80 nm), with crystallinity and elemental compositions of zinc (73.28%) and oxygen (20.48%), respectively. The ZnO NPs exhibited better antibacterial effects against Gram-positive bacteria (*Staphylococcus aureus* and *Bacillus subtilis*), compared to Gram-negative strains (*Escherichia coli* and *Pseudomonas aeruginosa*), as well as higher antifungal efficacy against *Aspergillus niger* than against *A. fumigatus*. Wound healing studies in albino mice demonstrated 98.13% wound closure by the 10^{th} day. Histopathology confirmed enhanced re-epithelialization, tissue regeneration, and collagen deposition in wounds treated with ZnO NPs. The findings highlight that *Mimosa pudica* mucilage (MPM) mediated ZnO NPs possess significant antimicrobial and wound healing potential, suggesting their suitability for future biomedical applications.

Keywords: *M. pudica*, mucilage, glucoxylan, wound healing, histopathology

INTRODUCTION

The skin is an essential organ in the human body, which plays a significant role in defending the body from harmful microbes. Frequently, skin wounds heal on their own or with little assistance.[1] The wound-healing progression is achieved in four vital steps: hemostasis, inflammation, proliferation, and maturation.[2] The healing of damaged tissues will be slowed down if any of the phases is interrupted. Several factors, including excessive granulation, excessive scar formation, and massive contraction, affect wound healing.[3] Infection by harmful bacteria colonizes the injured tissues, impeding and complicating the healing process. Therefore, there is an utmost demand to explore and develop new materials to heal infected wounds more quickly.[4]

The term “nanomaterials” describes materials with a large aspect ratio and one or more exterior dimensions between 1 and 100 nm. These can be nanolayers, nanotubes, and nanoparticles (NPs). Organic nanostructured substances include chitin whiskers, cellulose, lignocellulose, and starch nanocrystals, while inorganic nanostructured substances consist of carbon nanotubes, Ag, ZnO, Au, and TiO_2 NPs.[5] The metal NPs have been extensively explored due to their unique optical, catalytic,[6] magnetic, electrical,[7] wound healing, and antibacterial properties.[8] Prior studies have examined a range of potential uses for ZnO NPs.[9]

ZnO NPs have strong UV-A and UV-B absorption capabilities, which prevent them from scattering visible light, and provide them with a wide range of applications in products like sunscreen creams and cosmetics.[10] ZnO NPs have also been applied in agriculture, cancer treatment, antibacterial applications,[11] and wound healing.[12] ZnO NPs are produced using a variety of synthesis parameters, including laser ablation, microwave-assisted, sonochemical, lyophilization, solvothermal, chemical

vapor deposition, micro-emulsion, precipitation, and sol-gel combustion.[13] Apart from the traditional synthesis techniques, the environmentally friendly synthetic approach using biological plant extracts is easy, economical, reliable, and eco-friendly.[14] Many recent studies have examined the bio-reduction of various metal ions (Pt, Ag, Pd, and Au) into metal NPs.[15] A range of plant extracts, such as *Cotoneaster nummularia*,[16] *Euphorbia tirucalli*,[17] and lemon grass,[18] as well as biopolymers, like GX[19] and glucuronoxylan,[20] have been utilized in the environmentally friendly synthesis of NPs and their subsequent biological applications.[21]

M. pudica belongs to the *Mimosaceae* family and is native to Nigeria, America, Tanzania, Asia, Brazil, and the Pacific Islands.[22] The plant contains a variety of phytochemicals, including tannins, terpenoids, flavonoids, and sterols,[23] which may be responsible for treating conditions such as smallpox, ulcers, hemorrhoids, constipation, depression, inflammation, and snake bites.[24] *M. pudica* seeds were cleaned, soaked in water for 12 h, and then heated for 30 min at 50 °C to extract the MP mucilage (MPM) using cotton fabric. Previously, different techniques were used to analyze the material extracted from the MP seeds. The carbon, hydrogen, and nitrogen (CHN) elemental determination confirmed that on a dry-substance (anhydrous) basis, the isolated material's C and H percentages were 29.83 and 4.63, respectively. The material appears to be protein-free based on the lack of N.[25] Other naturally occurring polysaccharides have higher carbon and hydrogen values (45% C and 6.1% H), which may be due to a higher ash content.[26] The extracted substance was referred to as GX from MP, which is composed of glucose and xylose, based on their monosaccharide components. These findings show that the extracted substance is hemicellulose. According to current reports, glucose (30.89%) and xylose (69.11%) comprise the majority of MPM.[27] The major chain of MP consisted of β-1,4-*D*-xylose molecules, with glucose molecules connected through β-1,3-linkages, either in the branches or as a main chain component.[28] Based on this composition, mucilage extracted from MP seeds mainly consists of polysaccharides, playing a crucial role in NPs synthesis by serving as capping and reducing agents. In particular, seed mucilage has a viscous nature, which helps in inhibiting agglomeration by covering NPs.[29] In contrast, plant extracts, *e.g.* from leaves, might differ notably depending on aspects such as extraction techniques, growth conditions, and plant species. This diversity can lead to changes in the fabrication process and the features of synthesized NPs, making quality assurance and reliability challenging.[30] Several MPM applications include tablet binder, drug release, and water purification.[28]

To the authors' knowledge, it is the first report to synthesize ZnO NPs using mucilage extruded from the seeds of MP. The ZnO NPs were characterized using UV/Vis, FTIR, SEM, XRD, and EDX. The MPM-based ZnO NPs were investigated for antibacterial activity (zone of inhibition, minimum inhibitory concentrations, and minimum bactericidal concentrations) against the Gram-positive bacteria and Gram-negative bacteria mentioned above. The NPs were also explored for their potential against fungal strains (*A. fumigatus* and *A. nigar*). The wound-healing activity of ZnO NPs was evaluated in Albino mice, and re-epithelialization, tissue regeneration, and collagen synthesis were confirmed by histopathological analysis.

EXPERIMENTAL

Materials

MP seeds were acquired from a local shop near Government College University, Lahore, Pakistan. Analytical grade zinc acetate dihydrate was obtained from Merck. The Microbiology Department at Government College University, Lahore, provided fungal isolates and bacterial strains. Male albino mice were bought from the University of Veterinary and Animal Sciences, Lahore.

Extraction of MPM

The mucilage from the MP seeds was extracted by soaking the seeds (50 g) in distilled water (500 mL) for 20 min before heating for 2.0 h at 80 °C with continuous stirring. The viscous solution was cooled and filtered through cotton fabric to isolate MPM from the seeds. The isolated MPM was dried in an oven at 70 °C, ground to a fine powder, and stored in a vial for further experiments.

Synthesis of MPM-based ZnO NPs

The MPM suspension (2.0% in 10 mL of distilled water) and zinc acetate dihydrate (100 mM, 10 mL) were mixed and heated to 80 °C until the solution began to evaporate. After evaporating 80% of the water from the

mixture, it was transferred to a Petri dish and further dried in an oven at 80 °C. The white powder obtained after drying was calcined at 500 °C for 3 h to white MPM-based ZnO NPs.

Characterization

The UV analysis was performed using an Agilent Cary-60 spectrophotometer to assess the optical properties. The functional groups in MPM and ZnO NPs were analyzed using an FTIR spectrophotometer (Nicolet iS5 Spectrophotometer, Thermo Scientific, UK). The shape and size of the synthesized NPs were studied using a Nova-Nano SEM 450 equipped with EDX to determine the composition of ZnO NPs. Lastly, the XRD pattern (X'pert-MPD, PHILIPS) was analyzed to determine the crystalline structure of ZnO NPs using Cu Kα radiation (λ = 1.5418 Å).

Antimicrobial analysis

The agar well diffusion technique was used to evaluate the antimicrobial activity of NPs against various fungal and bacterial strains. Before making wells with a sterile cork borer, Muller-Hinton Agar (Merck, Germany) was applied to the Petri plates. The fungal and bacterial strains (according to the McFarland turbidity standard) were spread uniformly with cotton swabs. Out of four wells, two were filled with MPM-based ZnO NPs (50% and 100%), and two were filled with positive (ciprofloxacin in the case of bacterial and fluconazole in the case of fungal strains), and negative (distilled H_2O) controls. The Petri plates were incubated for 1 day at 37 °C, and the zone of inhibition (ZOI) was measured in mm.

MPM-based ZnO NPs in wound healing

To investigate the wound-healing performance of MPM-based ZnO NPs in male albino mice, EU directive ethical guidelines were followed.[31] Male albino mice with an average body weight of 100-150 g were supplied with regular food and water. Before shaving hair and creating wounds using a biopsy punch (5 mm in diameter) on the dorsal side, mice were injected with a combination of xylazine and ketamine to induce anesthesia. The mice were distributed into five groups, each group containing four mice. Group 1 was left untreated (NC), Group 2 was supplied with standard drug (PC), Group 3, containing alloxan-induced diabetic mice, was provided with the paste of MPM-based ZnO NPs, Group 4 with a paste of MPM, and Group 5, containing non-diabetic mice (normal animals), was also treated with MPM-based ZnO NPs, for 10 days. The animals were examined on days 3, 5, 7, and 10, and photographs were taken for visual comparison. The percentages of the wound contraction were determined using Equation 1:

$$\text{Wound closure (\%)} = \frac{\text{Diameter of wound on day 3} - \text{Diameter of wound on day 10}}{\text{Diameter of wound on day 3}} \times 100 \quad (1)$$

Mice in Group 3 were made diabetic after being injected with a dose of alloxan.[32] The mice were starved for the whole night before being given an intra-abdominal injection of alloxan monohydrate (0.25 mg/kg body weight). The mice were then given a regular diet for 24 h, along with a 10% glucose solution to prevent hypoglycemia. The mice's blood glucose levels were monitored, and diabetes was diagnosed after 24 h by measuring them with a glucometer. The mice's blood glucose level increased significantly to around 550 mg/dL after receiving alloxan, and these mice were used for additional testing.

To assess the toxicity of MPM and MPM-based ZnO NPs, a skin irritation test was conducted according to the reported procedure.[33] After removing hair, MPM and MPM-based ZnO NPs were pasted on the mice's skin, and unusual symptoms, such as irritation, dryness, or redness, were recorded at 2, 6, 24, and 48 h.

The present study is performed according to the existing literature showing the *in vitro* and *in vivo* biocompatibility of ZnO NPs.[34] Furthermore, all *in vivo* experiments are performed according to guidelines prescribed by the ethical committee, and the 3R principle (Replacement, Reduction, and Refinement) was followed strictly. The experimental design for animal use was approved by the Institutional Bioethics Committee (Ref. # GCU/IIB/270) at Government College University, Lahore, Pakistan. The study was conducted ethically in accordance with the ARRIVE guidelines and the U.K. Animals (Scientific Procedures) Act, 1986, as well as the associated guidelines and the EU Directive 2010/63/EU for animal experiments.

Histopathological analysis

The tissues from the wound area of all five groups were removed on the 10th day for histopathological analysis to determine cellular infiltration, epithelialization, collagen deposition, and angiogenesis. The separated tissues were fixed in 10% formalin and stained with hematoxylin and eosin for light microscopy. The slides were thoroughly prepared and analyzed.

RESULTS AND DISCUSSION

Synthesis of ZnO NPs

The synthesis of ZnO NPs was ensured by the noticeable change in the reaction mixture color that coincided with the reduction. After a 3 h treatment in a muffle furnace at 500 °C, white powder of

MPM-based ZnO NPs was obtained. Polysaccharides are unique substances used as reducing and capping agents for manufacturing NPs that require minimal reagents. In this regard, MP seeds contain GX, a mucilage-forming polysaccharide that can be isolated and used to synthesize ZnO NPs. Polysaccharide GX can serve as a stabilizing agent that helps to stabilize NPs.[35]

Characterization of ZnO NPs

UV-Visible spectroscopy

The dried seeds of MP, MPM, and dried mucilage obtained after drying liquid MPM at 70 °C are shown in Figure 1 (a-c). The MPM was further used to synthesize white-colored MPM-based ZnO NPs (Fig. 1d), and the optical property of the MPM-based ZnO NPs was determined by mixing NPs (1.0 mg) in distilled water (10 mL). Figure 1 (e) shows the absorption band for the synthesized MPM-based ZnO NPs in the wavelength range of 200 to 800 nm, and due to the inter-band transition of electrons, a prominent peak at 390 nm appears, which indicates the successful production of MPM-based ZnO NPs. Previous studies reported that ZnO NPs from quince seed mucilage show a peak at 384 nm,[36] from *Nyctanthes arbor-tristis* at 370 nm[37] and psyllium mucilage at 364 nm.[12] The band gap energy value of synthesized NPs was also calculated using the following equation:

$$E_{bg} = \frac{hc}{\lambda} \qquad (2)$$

The value of E_{bg} was 3.18 eV, which was close to the previously reported values.[36,12]

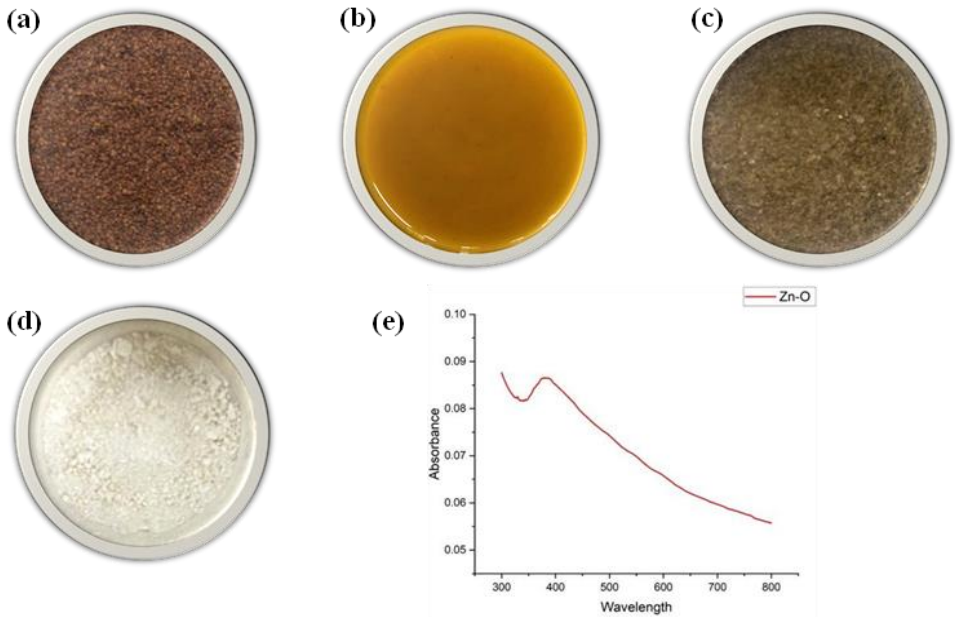

Figure 1: (a) MP seeds, (b) Mucilage isolated from MP seeds, (c) Dried mucilage of MP, (d) ZnO NPs synthesized from MPM, (e) UV/Vis spectrum of MPM-based ZnO NPs

FTIR spectroscopy

Several functional groups of MPM, acting as capping and reducing agents, were identified by FTIR analysis. The FTIR spectra of MPM and MPM-based ZnO NPs are presented in Figure 2. The FTIR spectrum of MPM indicates peaks at different wavenumbers: 3294 cm^{-1} due to -OH stretching, 2950 cm^{-1} due to C-H stretching, 1585 cm^{-1} linked to C=O, 1395 cm^{-1} due to C-H bending vibration, and 1028 cm^{-1} related to C-O-C stretching vibration. In the spectrum of MPM-based ZnO, the peak at 3386 cm^{-1} is due to the -OH stretching, and 2977 cm^{-1} is due to the C-H stretching. A peak at 1542 cm^{-1} is related to the C=O, while a peak at 1023 cm^{-1} is linked to the C-O-C group. A sharp peak near 688 cm^{-1} is associated with the $Zn(OH)_2$ bond. The region between 400 and 600 cm^{-1} is assigned to the metal-oxygen bond, and two peaks near 484 and 441 cm^{-1} confirm the synthesis of ZnO NPs, which agrees with the results reported in the literature.[38,35]

Morphological studies

Essential details about the size, distribution, aggregation, and surface appearance of NPs are provided by SEM.[39] More magnified images illustrate the ideal dimensions and shapes of NPs. The ZnO NPs synthesized from MPM are mostly spherical, as demonstrated by SEM micrographs (Fig. 3), with minor agglomeration likely due to the van der Waals forces. Numerous studies propose that agglomeration can be ascribed to various factors in the synthesis process, including variations in the medium's pH and temperature, high surface area, polarity, and phytochemical moieties present on the surface of biologically synthesized NPs.[40] Several studies have reported that, at lower precursor concentrations, ZnO NPs have a spherical shape. At higher concentrations, cubical and hexagonal-shaped particles are also obtained.[41] The average diameter of ZnO NPs was 51.80 nm, calculated using ImageJ software (Fig. 4).

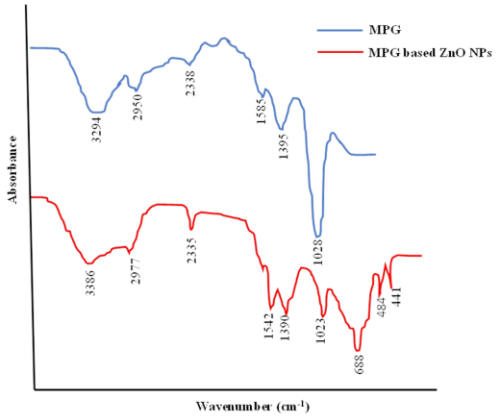

Figure 2: Comparison between FTIR spectra of MPM and MPM-based ZnO NPs

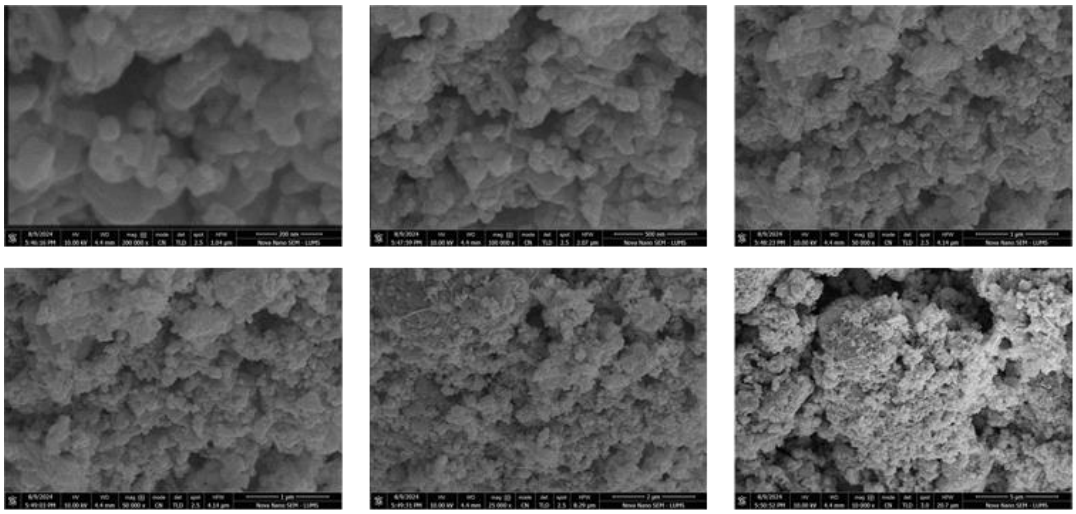

Figure 3: SEM images of MPM-based ZnO NPs at different magnifications

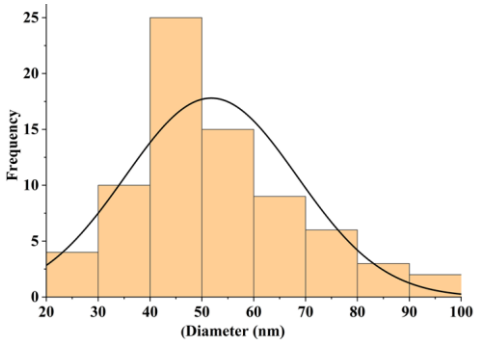

Figure 4: Average particle size of MPM-based ZnO NPs

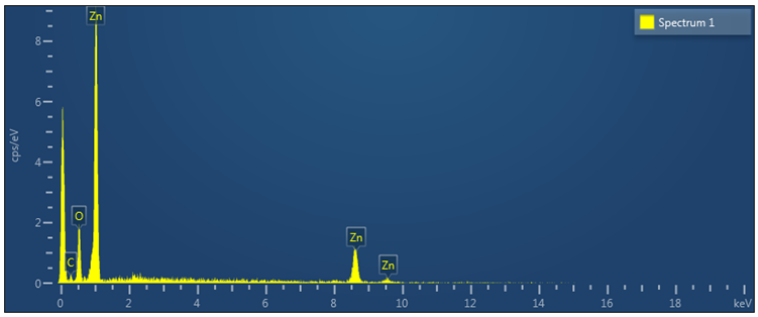

Figure 5: EDX spectrum of MPM-based ZnO showing the composition of the synthesized NPs

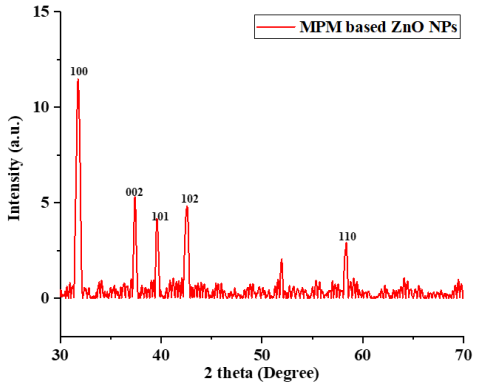

Figure 6: XRD pattern of MPM-based ZnO NPs

EDX analysis

EDX demonstrated the elemental composition, impurities present, and relative abundance of elements in ZnO NPs.[39] According to the EDX spectrum, the MPM-based ZnO NPs have the desired elemental composition of Zn and O, with carbon (Fig. 5). In the EDX spectrum, the presence of zinc and oxygen peaks confirmed the presence of ZnO NPs. The results are similar to the previous studies.[42,43] The MPM-based ZnO NPs have a composition of 73.28% Zn and 20.48% O, which closely aligns with prior studies.[44]

XRD pattern and phase analysis

The XRD peaks confirmed the presence of ZnO crystallites. The analysis revealed no extra signals, indicating the homogeneity of the MPG-based ZnO NPs. The diffraction peak positions are matched with those reported for the JCPDS Standard (36-1451). The values of 2θ (degrees) at 31.76°, 37.42°, 39.5°, 42.54°, and 58.21° correspond to the ZnO NPs diffraction peaks at 100, 002, 101, 102, and 110, respectively, with a hexagonal structure (Fig. 6). These results are mostly consistent with the reported results.[45]

Biological applications

Antibacterial investigation

The agar well diffusion technique was used to assess the bactericidal potential of MPM-based ZnO NPs against various bacterial strains (Gram-positive and Gram-negative). Research has shown that NPs are effective against a wide range of bacteria. The ZOI values against Gram-positive bacteria, *i.e.*, 17.53 ± 0.03 mm (*B. subtilis*) and 15.57 ± 0.13 mm (*S. aureus*) with pure NPs, were higher (Fig. 7) than those against Gram-negative bacteria, *i.e.*, 13.52 ± 0.07 mm (*P. aeruginosa*) and 14.6 ± 0.08 mm (*E. coli*). The negative control (distilled water) showed no ZOI value, and the results were comparable to those of the positive control, ciprofloxacin. Premanathan *et al.*[46] also reported that compared to Gram-negative bacteria (*E. coli* and *P. aeruginosa*), Gram-positive bacteria (*S. aureus*) are more susceptible to ZnO NPs due to variations in the cell wall structure. Zhang *et al.*[47] provided strong support by speculating that ZnO NP's antibacterial action might result from their capacity to penetrate bacterial cell membranes. The charges present on the surface of NPs and the electrostatic attraction between NPs and bacterial surfaces are the reasons that cause the NPs to come into contact with

bacterial cells.[48] Zhang *et al*. employed electrochemical tests to verify that ZnO NPs in contact with bacterial membranes generated a high concentration of reactive oxygen species, leading to bacterial death due to chemical reactions between membrane proteins and hydrogen peroxide.[49]

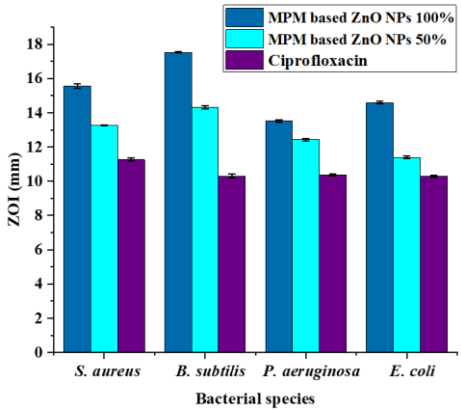

Figure 7: ZOI graph of MPM-based ZnO NPs against different gram-positive and gram-negative bacterial strains

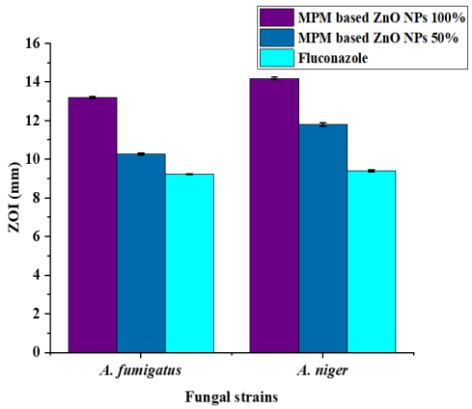

Figure 8: ZOI values of MPM-based ZnO NPs against two fungal strains

Antifungal investigation

The antifungal potential of different concentrations of ZnO NPs was assessed against two fungal strains (*A. fumigatus* and *A. niger*) using the disc diffusion method. The antifungal efficacy was dose-dependent, increasing with NP concentration. At higher NP concentrations, the ZOI values were higher than the standard drug, fluconazole (Fig. 8). The interaction between NPs and the fungal cell wall may be the cause of the clear and large ZOI. NPs generate reactive oxygen species that kill the fungal strain. ZnO NPs synthesized using biofabricated methods exhibit antifungal properties and are widely utilized in bioactive food packaging materials.[50]

Wound healing potential

Healing has several facets and can progress or regress depending on factors such as the patient's internal and external environment.[51] The main components for rational treatment decisions are the therapeutic effect, dosage, depth, and different techniques. Researchers have been seeking technologies to eliminate microbes and maintain a moist environment.[52] Natural polymers with significant biological functions can be used for this purpose.[53] Collagen helps keep tissues moist and protected during the repair process.[54] Another protein that assists in stopping bleeding is fibrin, which is accomplished by entrapping platelets as the primary clot forms.[55]

The mucilages combined with NPs exhibit enhanced efficacy, making wound dressings more practical. The incorporation of NPs into mucilages has enhanced their adhesion properties and drug-delivery efficacy through covalent coupling and non-covalent interactions. Henceforth, it is possible to apply nanomucilages directly to the wound to promote healing and stimulate the development of new capillaries and hair follicles.[56] Compared to standard formulations, certain mucilage functionalities have improved pharmacological healing potential. The primary characteristics of mucilage-based dressings include antibacterial, self-healing, targeted delivery, hemostatic, surface adhesion, stimuli-responsive, antioxidant, and anti-inflammatory properties.[57]

Considering the high surface area/volume ratio, NPs are a good choice for the healing of wounds. Due to their remarkable properties, such as their ability to stimulate wound healing and exhibit antimicrobial activity, metal NPs, including Zn, Au, and Ag, could be used in wound dressings to improve their effectiveness.[58] ZnO NPs show promise as an effective antibacterial agent when added to mucilage-based wound dressings because they cause bacterial cell membrane perforations, which in turn encourage keratinocyte migration and enhance re-epithelialization by extending the contact time.[59] Furthermore, the re-epithelialization and antibacterial properties of biopolymeric NPs as wound treatments or delivery systems are remarkable.[60] Wound contraction reflects the rate at which unhealed areas are reduced following treatment. The greater the reduction, the more effective the drug. In this study, the wound-healing potential of ZnO NPs was investigated, and the results were compared with

those of four groups of mice receiving other treatments. To visually interpret the impact of MPM-based ZnO NPs, the photographs were taken on alternate days (1st, 5th, and 10th) (Fig. 9a).

The percentage of wound contraction indicated that the mice in Group 5, which received treatment with MPM-based ZnO NPs, exhibited better wound healing, higher wound contraction, and improved skin appearance, as well as normal hair development, compared to the other groups. On the 10th day after infection, the study found that ZnO NPs induced wound healing by 98.13% in Group 5 and 50.80% in Group 3 (the diabetic group). Group 4 treated with MPM showed wound contraction of about 75.83%, and the control groups (1 and 2) showed 45.93% and 66.03%, respectively (Fig. 9b). ZnO NPs accelerate the formation of new collagen and cause the lesion to shrink, resulting in a comparatively smaller scar.[61] They can also control insulin-like growth factor I and endogenous growth hormone, which may promote epithelialization.[62] ZnO NPs improve debris clearance, re-epithelialization, platelet activation, and angiogenesis. ZnO NPs can effectively and aesthetically heal wounds, and they can also function as antibacterial tissue adhesives. Zinc oxide (ZnO) promotes collagen deposition by encouraging more fibroblasts to migrate to the wound site.[63] Zinc ions are thought to be responsible for ZnO NPs' healing properties because they promote re-epithelialization by causing keratinocyte migration to the location of the wound. These results indicate that ZnO NPs synthesized using MPM can swiftly heal wounds and potentially replace existing antibiotics.

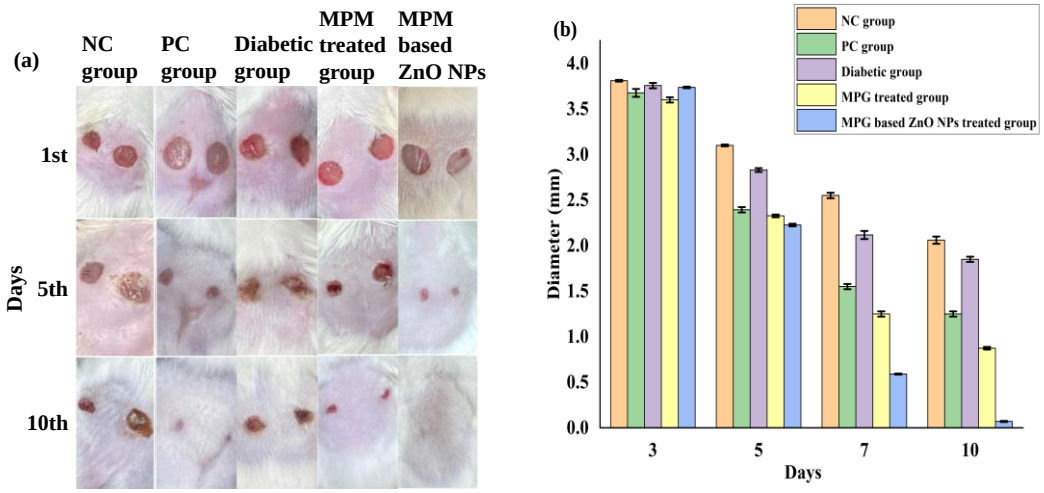

Figure 9: (a) Photographs taken on alternate days after wound insertion, (b) Diameter of the wound closure on different days

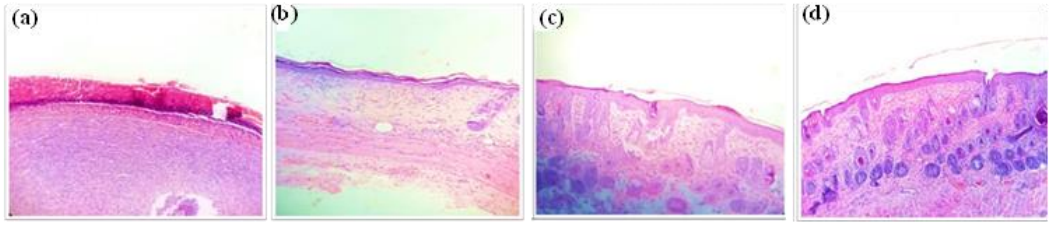

Figure 10: Histopathological analysis of (a) control group, (b) diabetic group, (c) MPM-treated group, (d) MPM-based ZnO NPs treated group

Histopathological analysis (Fig. 10) revealed that mice treated with NPs and MPM exhibited better wound closure compared to the control and diabetic groups. Histopathology of tissue removed on the 10th day (Group 2) revealed rapid restoration of the skin at the wound site, characterized by an increase in collagen fibers, resulting in enhanced tissue strength. Complete re-epithelialization was observed in this group, indicating a smoother healing process. The mice treated with the MPM paste showed more noticeable results than the control and diabetic groups. The MPM paste stimulated re-epithelialization, tissue regeneration, and collagen synthesis. The histopathological analysis of the diabetic group revealed the slowest healing rate among all groups, attributed to difficulties in re-epithelialization, reduced cross-linking between collagen fibers, and prolonged tissue regeneration. Various metabolic

factors, such as elevated blood sugar levels, can disrupt wound healing and compromise tissue structural stability.

CONCLUSION

ZnO NPs can be synthesized from MP seed extrudates, an environmentally friendly technique with several advantages over traditional methods. The UV/VIS analysis was the first step, which indicates the formation of ZnO NPs. Other analytical techniques, including FTIR, confirmed the role of capping agents in the synthesis of ZnO NPs. SEM micrographs confirmed that most particles were spherical with little agglomeration, EDX revealed the composition, and XRD phases confirmed the hexagonal structure of the synthesized ZnO NPs. ZnO NPs synthesized from MPM exhibited antibacterial and antifungal activity, and satisfactory results were obtained. The role of MPM-based ZnO NPs in wound healing was also evaluated, and the results confirmed that 98.13% of the wound was healed on day 10. These results suggested that MPM-based ZnO NPs can be used effectively in biomedical applications.

REFERENCES

[1] S. N. Nandhini, N. Sisubalan, A. Vijayan, C. Karthikeyan, M. Gnanaraj *et al*., *Heliyon*, **9**, e15327 (2023), https://doi.org/10.1016/j.heliyon.2023.e13128

[2] T. Velnar, T. Bailey and V. Smrkolj, *J. Int. Med. Res*., **37**, 1528 (2009), https://doi.org/10.1177/147323000903700531

[3] M. Batool, S. Khurshid, Z. Qureshi and W. M. Daoush, *Chem. Pap*., **75**, 893 (2021), https://doi.org/10.1007/s11696-020-01343-7

[4] M. H. Teaima, M. K. Elasaly, S. A. Omar, M. A. El-Nabarawi and K. R. Shoueir, *J. Drug Deliv. Sci. Technol*., **67**, 102982 (2022), https://doi.org/10.1016/j.jddst.2021.102982

[5] B. Ghanbarzadeh, S. A. Oleyaei and H. Almasi, *Crit. Rev. Food Sci. Nutr*., **55**, 1699 (2015), https://doi.org/10.1080/10408398.2012.731023

[6] A. Majeed, G. Muhammad, M. R. Raza, M. Amin, A. Afzal *et al*., *Cellulose Chem. Technol*., **59**, 1033 (2025), https://doi.org/10.35812/CelluloseChemTechnol.2025.59.86

[7] N. Durán, P. D. Marcato, O. L. Alves, G. I. H. de Souza and E. Esposito, *J. Nanobiotechnol*., **3**, 8 (2005), https://doi.org/10.1186/1477-3155-3-8

[8] M. A. Hussain, A. Shaheen, S. Z. Hussain, I. Hussain, M. T. Haseeb *et al*., *Cellulose Chem. Technol*., **57**, 993 (2023), https://doi.org/10.35812/CelluloseChemTechnol.2023.57.87

[9] M. Chennimalai, V. Vijayalakshmi, T. S. Senthil and N. Sivakumar, *Mater. Today Proc*., **47**, 1842 (2021), https://doi.org/10.1016/j.matpr.2021.03.409

[10] K. Schilling, B. Bradford, D. Castelli, E. Dufour and J. F. Nash, *Photochem. Photobiol. Sci*., **9**, 495 (2010), https://doi.org/10.1039/b9pp00180h

[11] N. A. abd El Ghany, N. A. Mohamed and Z. M. Mahmoud, *Cellulose Chem. Technol*., **59**, 841 (2025), https://doi.org/10.35812/CelluloseChemTechnol.2025.59.71

[12] A. Azam, G. Muhammad, M. S. Aslam, M. M. Iqbal and M. A. Raza, *Appl. Organomet. Chem*., **37**, e6923 (2023), https://doi.org/10.1002/aoc.6923

[13] B. Bhuyan, B. Paul, D. D. Purkayastha, S. S. Dhar and S. Behera, *Mater. Lett*., **168**, 158 (2016), https://doi.org/10.1016/j.matlet.2016.01.024

[14] G. Hosseinzadeh, S. Zinatloo-Ajabshir and A. Yousefi, *Ceram. Int*., **48**, 6078 (2022), https://doi.org/10.1016/j.ceramint.2021.11.146

[15] Y. Govender, T. L. Riddin, M. Gericke and C. G. Whiteley, *J. Nanopart. Res*., **12**, 261 (2010), https://doi.org/10.1007/s11051-009-9604-3

[16] N. Asad, M. Naeem-ul-Hassan, M. A. Hussain, A. Abbas, M. Sher *et al*., *Nat. Prod. Res*., **1**, 15 (2023), https://doi.org/10.1080/14786419.2023.2295936

[17] B. S. Ravikumar, H. Nagabhushana, D. V. Sunitha, S. C. Sharma, B. M. Nagabhushana *et al*., *J. Alloys Compd*., **585**, 561 (2014), https://doi.org/10.1016/j.jallcom.2013.09.080

[18] S. S. Shankar, A. Rai, B. Ankamwar, A. Singh, A. Ahmad *et al*., *Nat. Mater*., **3**, 482 (2004), https://doi.org/10.1038/nmat1152

[19] Tuba, S. Javed, M. R. Raza, M. U. Sharif, A. Majeed *et al*., *Desalin. Water Treat*., **2024**, 100388 (2024), https://doi.org/10.1016/j.dwt.2024.100388

[20] G. Muhammad, M. A. Hussain, M. Amin, S. Z. Hussain, I. Hussain *et al*., *RSC Adv*., **7**, 42900 (2017), https://doi.org/10.1039/C7RA07555C

[21] A. Arshad, M. A. Hussain, M. T. Haseeb, S. N. Abbas Bukhari, G. Muhammad *et al*., *Curr. Drug Deliv*., **20**, 292 (2023), https://doi.org/10.2174/1567201819666220509200019

[22] G. Muhammad, M. A. Hussain, I. Jantan and S. N. A. Bukhari, *Compr. Rev. Food Sci. Food Saf*., **15**, 303 (2016), https://doi.org/10.1111/1541-4337.12184

[23] E. N. Bum, D. L. Dawack, M. Schmutz, A. Rakotonirina, S. V. Rakotonirina *et al*., *Fitoterapia*, **75**, 309 (2004), https://doi.org/10.1016/j.fitote.2004.01.012
[24] K. S. Girish, H. P. Mohanakumari, S. Nagaraju, B. S. Vishwanath and K. Kemparaju, *Fitoterapia*, **75**, 378 (2004), https://doi.org/10.1016/j.fitote.2004.01.006
[25] F. Iram, S. Massey, M. S. Iqbal and D. G. Ward, *J. Carbohyd. Chem*., **37**, 285 (2018), https://doi.org/10.1080/07328303.2018.1487973
[26] R. A. Laidlaw and E. G. V. Percival, *J. Chem. Soc*., 528 (1950), https://doi.org/10.1039/JR9500000528
[27] S. Massey, M. S. Iqbal, B. Wolf, I. Mariam and S. Rao, *Lat. Am. J. Pharm*., **35**, 146 (2016)
[28] G. Muhammad, M. U. Ashraf, M. Naeem-ul-Hassan and S. N. A. Bukhari, *Braz. J. Pharm. Sci*., **54**, e00032 (2018), https://doi.org/10.1590/s2175-97902018000317579
[29] N. U. Rehman, G. Muhammad, M. U. Sharif and M. A. Hussain, *Desalin. Water Treat*., **320**, 100853 (2024), https://doi.org/10.1016/j.dwt.2024.100853
[30] S. Kazemi, A. Hosseingholian, S. D. Gohari, F. Feirahi, F. Moammeri *et al*., *Mater. Today Sustain*., **24**, 100500 (2023), https://doi.org/10.1016/j.mtsust.2023.100500
[31] I. A. S. Olsson, S. P. da Silva, D. Townend and P. Sandøe, *ILAR J*., **57**, 347 (2017), https://doi.org/10.1093/ilar/ilw029
[32] S. Lenzen, *Diabetologia*, **51**, 216 (2008), https://doi.org/10.1007/s00125-007-0886-7
[33] N. Mohamad, M. C. I. M. Amin, M. Pandey, N. Ahmad and N. F. Rajab, *Carbohyd. Polym*., **114**, 312 (2014), https://doi.org/10.1016/j.carbpol.2014.08.025
[34] Y. Zheng, R. Li and Y. Wang, *Int. J. Mod. Phys. B*, **23**, 1566 (2009), https://doi.org/doi.org/10.1142/S0217979209061275
[35] R. Acharya, F. Tettey, A. Gupta, K. R. Sharma, N. Parajuli *et al*., *Discov. Appl. Sci*., **6**, 85 (2024), https://doi.org/10.1007/s42452-024-05719-2
[36] S. M. T. H. Moghaddas, B. Elahi and V. Javanbakht, *J. Alloys Compd*., **821**, 153519 (2020), https://doi.org/10.1016/j.jallcom.2019.153519
[37] N. Rani, S. Rani, H. Patel, S. Yadav, M. Saini *et al*., *Inorg. Chem. Commun*., **150**, 110516 (2023), https://doi.org/10.1016/j.inoche.2023.110516
[38] R. Gomathi and H. Suhana, *Inorg. Nano-Met. Chem*., **51**, 1663 (2021), https://doi.org/10.1080/24701556.2020.1852256
[39] S. Dawadi, S. Katuwal, A. Gupta, U. Lamichhane, R. Thapa *et al*., *J. Nanomater*., **2021**, 6687290 (2021), https://doi.org/10.1155/2021/6687290
[40] A. Sajjad, S. H. Bhatti, Z. Ali, G. H. Jaffari, N. A. Khan *et al*., *ACS Omega*, **6**, 11783 (2021), https://doi.org/10.1021/acsomega.1c01512
[41] A. R. Maheo, B. S. M. Vithiya, T. A. Arul Prasad, V. L. Mangesh, T. Perumal *et al*., *ACS Omega*, **8**, 10954 (2023), https://doi.org/10.1021/acsomega.2c07530
[42] A. A. Barzinjy and H. H. Azeez, *SN Appl. Sci*., **2**, 991 (2020), https://doi.org/10.1007/s42452-020-2813-1
[43] S. K. Chaudhuri and L. Malodia, *Appl. Nanosci*., **7**, 501 (2017), https://doi.org/10.1007/s13204-017-0586-7
[44] L. P. Chandrasekar, B. D. Sethuraman, M. Subramani and S. Mohandos, *Int. J. Environ. Anal. Chem*., **1**, 18 (2023), https://doi.org/10.1080/03067319.2023.2190458
[45] C. R. Mendes, G. Dilarri, C. F. Forsan, V. M. R. Sapata, P. R. M. Lopes *et al*., *Sci. Rep*., **12**, 2658 (2022), https://doi.org/10.1038/s41598-022-06657-y
[46] M. Premanathan, K. Karthikeyan, K. Jeyasubramanian and G. Manivannan, *Nanomedicine*, **7**, 184 (2011), https://doi.org/10.1016/j.nano.2010.10.001
[47] L. Zhang, Y. Jiang, Y. Ding, M. Povey and D. York, *J. Nanopart. Res*., **9**, 479 (2007), https://doi.org/10.1007/s11051-006-9150-1
[48] P. K. Stoimenov, R. L. Klinger, G. L. Marchin and K. J. Klabunde, *Langmuir*, **18**, 6679 (2002), https://doi.org/10.1021/la0202374
[49] L. Zhang, Y. Jiang, Y. Ding, N. Daskalakis, L. Jeuken *et al*., *J. Nanopart. Res*., **12**, 1625 (2010), https://doi.org/ 10.1007/s11051-009-9711-1
[50] M. A. Abomuti, E. Y. Danish, A. Firoz, N. Hasan and M. A. Malik, *Biology*, **10**, 1075 (2021), https://doi.org/10.3390/biology10111075
[51] N. Desai, D. Rana, S. Salave, R. Gupta, P. Patel *et al*., *Pharmaceutics*, **15**, 1313 (2023), https://doi.org/10.3390/pharmaceutics15041313
[52] M. Bao, K. Wang, J. Li, Y. Li, H. Zhu *et al*., *Acta Biomater*., **161**, 250 (2023), https://doi.org/10.1016/j.actbio.2023.02.026
[53] J. Wang, Y. Liu, Y. Liu, H. Huang, S. Roy *et al*., *J. Control. Release*, **353**, 563 (2023), https://doi.org/10.1016/j.jconrel.2022.11.057
[54] A. Tonelli, E. N. Lumngwena and N. A. B. Ntusi, *Nat. Rev. Cardiol*., **20**, 386 (2023), https://doi.org/10.1038/s41569-022-00825-3

[55] F. Zhang, Z. Xu and K. J. Jolly, *Adv. Drug Deliv. Rev.*, **197**, 114827 (2023), https://doi.org/10.1016/j.addr.2023.114827
[56] Y. Liu, S. Song, S. Liu, X. Zhu and P. Wang, *J. Nanomater.*, **2022**, 4656037 (2022), https://doi.org/10.1155/2022/4656037
[57] Y. Liang, J. He and B. Guo, *ACS Nano*, **15**, 12687 (2021), https://doi.org/10.1021/acsnano.1c04206
[58] Y. Zhang, Y. Zhu, P. Ma, H. Wu, D. Xiao *et al.*, *Carbohyd. Polym.*, **312**, 120823 (2023), https://doi.org/10.1016/j.carbpol.2023.120823
[59] Z. Li, X. Zhang, Y. Gao, Y. Song, M. X. Sands *et al.*, *Adv. Healthc. Mater.*, **12**, 2202770 (2023), https://doi.org/10.1002/adhm.202202770
[60] K. Huanbutta, W. Sittikijyothin and T. Sangnim, *J. Pharm. Investig.*, **50**, 625 (2020), https://doi.org/10.1007/s40005-020-00493-w
[61] Z. Saremi, R. Yari, I. Khodadadi and S. M. Tabatabaei, *J. Skin Stem Cell*, 3 (2016), https://doi.org/10.5812/jssc.66329
[62] K. Arslan, O. Karahan, A. Okus, Y. Unlu, M. A. Eryilmaz *et al.*, *Ulus. Travma Acil Cerrahi Derg.*, **18**, 376 (2012), https://doi.org/10.5505/tjtes.2012.45381
[63] P. T. Sudheesh Kumar, V.-K. Lakshmanan, M. Raj, R. Biswas, T. Hiroshi *et al.*, *Pharm. Res.*, **30**, 523 (2013), https://doi.org/10.1007/s11095-012-0898-y